A Simple Model for the Hygroscopy of Sulphuric Acid

Kristian B. Kiradjiev,[*,†] Vladimiros Nikolakis,[‡] Ian M. Griffiths,[†] Uwe Beuscher,[‡]

Vasudevan Venkateshwaran,[‡] and Christopher J. W. Breward[†]

†*Mathematical Institute, University of Oxford, Woodstock Rd, OX2 6GG, Oxford, UK*

‡*W. L. Gore and Associates, Inc., 100 Airport Rd, Elkton, MD 21921, USA*

E-mail: kristian.kiradjiev@maths.ox.ac.uk

Abstract

Sulphuric acid is a highly hygroscopic substance, increasing its volume by absorbing water from high relative-humidity environment. In this paper, we present a mathematical model that describes the hygroscopy of a uniform layer of sulphuric acid with a given initial concentration and relative humidity of the surrounding gaseous environment. We assume that water is absorbed across the gas–liquid interface at a rate proportional to the difference in concentration from the equilibrium value. Our numerical results compare well with asymptotic predictions for small Sherwood number, where we derive an explicit solution. The theory agrees well with experimental data, which supports the validity of the model, and we are able to use the model to determine the rate of absorption, which cannot be found by a direct experimental measurement.

1 Introduction

Sulphuric acid is used in a wide range of industrial applications, including as a catalyst in alkylation reactions, in petroleum refining, in the manufacture of detergents, and as an

important component in lead-acid batteries[1]. Sulphuric acid can be produced as a by-product, for example, when removing sulphur dioxide from flue gas. Its properties have been extensively studied and established empirically[2–4]. A prominent feature of sulphuric acid is its hygroscopy, i.e., its tendency to absorb water vapour from its surroundings[1]. When water vapour is absorbed, the volume of the sulphuric acid solution increases and consequently dilutes the acid concentration.

Water absorption into liquids has been well studied and modelled[5,6] as far as the mechanism of the process at the gas–liquid interface is concerned. In Lewis and Whitman[5], and Greenewalt[6], they describe the principles of gas absorption in terms of a "two-film" theory, in which thin stationary films of the corresponding phase on either side of the interface are assumed to exist which provide resistance to mass transfer. The absorptive flux depends linearly on the difference between the concentration of water at the gas–liquid interface and the equilibrium value of the concentration of water in the liquid when there is no net absorption.

The hygroscopic growth of materials has been mainly considered in the context of swelling of solid porous materials such as mortar, polymers and powders[7–10] rather than aqueous solutions such as aqueous sulphuric acid. In Delgado et al.[8], they present a model for the hygroscopic material that uses a non-linear expression for the rate of increase of water content that has a power-law dependence on the difference between the amount of water at the surface and at equilibrium. However, their model assumes that the water is well mixed in the bulk, and so does not incorporate water transport across the material.

A conservation-of-mass type of model for hygroscopic swelling of porous spherical particles, which incorporates the diffusive transport of water, is presented in Sweijen et al.[11]. They track the volume fraction of water and model absorption at the interface as a first-order kinetics process. Furthermore, they investigate numerically the regimes when diffusion and water absorption dominate, respectively, and derive a formula for the particle radius as a function of the water volume fraction. In this model, the water fraction at the particle surface is assumed to be independent of diffusion processes in the bulk and is solved for

separately to obtain an exponential evolution in time. This makes the boundary condition at the surface of the particle a time-dependent Dirichlet condition.

Hennessy et al.[12] develop a model for solvent evaporation and adsorption in thin liquid films. They track the volume fraction of the solvent using a nonlinear diffusion model, couple this with mass transfer across the moving interface, and fit solutions of their model against experimental data from ternary solutions, to find the mass transfer coefficient for their systems. We will use a simplified version of their model in this paper in which we set the diffusivity to be constant and track the concentration, rather than volume fraction, of water in the liquid layer. Similar models for solvent diffusion in glassy polymers are presented in Alfrey et al.[13], Cohen and Erneux[14], Mitchell and O'Brien[15].

We want to quantify the hygroscopy effect in layers of sulphuric acid produced in purification devices that remove sulphur dioxide from flue gas. In these devices, water vapour is absorbed from the flue gas by the sulphuric acid layers that grow around the microscopic device surfaces. The additional volume attributed to hygroscopy further reduces device efficiency and leads to swifter clogging. Understanding the amount of moisture uptake in such devices is crucial in understanding their performance and the time it takes for them to clog. However, the fundamental parameter controlling hygroscopy, the mass transfer coefficient associated with water transport across the interface, is not readily available in the literature. Thus, in this paper, we will follow Hennessy et al.[12] and present a simple mathematical model to describe the hygroscopy of a layer of sulphuric acid, compare the solutions to the model against experimental data, and determine this coefficient. Unlike Delgado et al.[8], we will incorporate diffusion of water, and, therefore, track the spatially non-uniform water concentration in the sulphuric acid. In addition, we do not calculate the water concentration at the gas–liquid interface separately, as in Sweijen et al.[11], but couple it with the diffusion process in the bulk of the solution. The plan for the paper is as follows. In §2, we will present the governing equations and boundary and initial conditions that describe the concentration of water in a layer of aqueous sulphuric acid with thickness that can change as

water is absorbed. In §2.2, we will non-dimensionalise the model, and introduce three key dimensionless parameters. In §2.3, we consider a distinguished limit of the model in which diffusion is the dominating process. In §3, we will describe the corresponding experiments. We will present numerical results, compare these with asymptotic results and experimental data, and determine the mass transfer coefficient in §4. Finally, we will draw conclusions in §5.

2 Mathematical Model

We consider a liquid layer of sulphuric acid residing on an impermeable substrate, with its upper surface exposed to an atmosphere containing water at a constant relative humidity, as shown in figure 1. We suppose that the liquid film has initial thickness $\hat{x} = \hat{h}_0$ (measured in m) and contains water with concentration $\hat{c}_0$ (measured in $\mathrm{mol\,m^{-3}}$). Across the gas–liquid interface, we assume that the flux of water into the film, $\hat{Q}$ (measured in $\mathrm{mol\,m^{-2}\,s^{-1}}$), caused by the hygroscopy of the sulphuric acid, is proportional to the difference between the concentration of dissolved water at the gas–liquid interface and the equilibrium concentration, $\hat{c}_{\mathrm{eq}}$, which is the concentration of water in the sulphuric acid associated with a balance in chemical potentials across the interface at a given relative humidity. For simplicity, we assume that this relationship is linear in the concentration difference and thus we write $\hat{Q} = \hat{k}(\hat{c}|_{\hat{x}=\hat{h}} - \hat{c}_{\mathrm{eq}})$, where $\hat{k}$ (measured in $\mathrm{m\,s^{-1}}$) is the mass transfer coefficient associated with water absorption, assumed to be constant.

In practice, $\hat{c}_{\mathrm{eq}}$ can be experimentally determined[16] and depends on the relative humidity and temperature of the surrounding air. For simplicity, we assume isothermal conditions so that $\hat{c}_{\mathrm{eq}}$ is a constant. In the liquid film, we assume that water is transported by diffusion with constant diffusivity $\hat{D}$ (measured in $\mathrm{m^2\,s^{-1}}$), and that volume changes due to mixing are negligible. In practice, the diffusivity may vary with concentration but we will find that, for the parameter regime of interest, this does not play a role, while for other regimes, which

we consider in the Supplementary Information, we will show that a concentration-dependent diffusivity has a minimal effect on the behaviour.

We also note that, since the water vapour absorbed at the top of the liquid film is less dense than the sulphuric acid, convective effects due to density variations are negligble. Given that we expect the surface tension of the liquid layer to keep the air–liquid interface flat, we restrict ourselves to a one-dimensional model with changes only occuring in the vertical direction. Of course, small menisci exist at the edges of the layer, but we anticipate that their influence will be confined to a small boundary layer near the walls and expect that these will have negligible effect on the mass transfer. Thus, we obtain the following model for the water concentration within the film, $\hat{c}$, and the thickness of the film, $\hat{h}$,

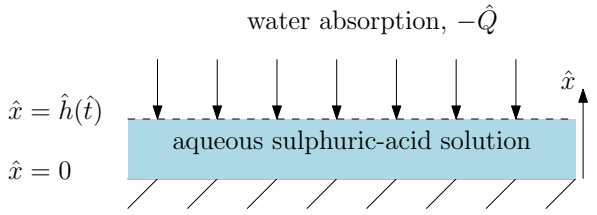

Figure 1: Schematic of the model system.

$$\frac{\partial \hat{c}}{\partial \hat{t}} = \hat{D}\frac{\partial^2 \hat{c}}{\partial \hat{x}^2}, \tag{1}$$

$$\frac{\mathrm{d}\hat{h}}{\mathrm{d}\hat{t}} = \hat{k}\hat{V}_m(\hat{c}_{\mathrm{eq}} - \hat{c}|_{\hat{x}=\hat{h}}), \tag{2}$$

where $\hat{V}_m$ (measured in $\mathrm{m}^3\,\mathrm{mol}^{-1}$) is the molar volume of water.

At the gas–liquid interface, we conserve flux relative to the moving interface and write

$$-\hat{D}\frac{\partial \hat{c}}{\partial \hat{x}} - \hat{c}\frac{\mathrm{d}\hat{h}}{\mathrm{d}\hat{t}} = \hat{k}(\hat{c} - \hat{c}_{\mathrm{eq}}) \qquad \text{at} \qquad \hat{x} = \hat{h}(\hat{t}). \tag{3}$$

At the surface of the substrate, $\hat{x} = 0$, we impose no flux of water, and, thus, we write

$$-\hat{D}\frac{\partial \hat{c}}{\partial \hat{x}} = 0 \qquad \text{at} \qquad \hat{x} = 0. \tag{4}$$

We assume that, initially, the concentration of water is known and uniform, and that the thickness of the film is given, and, thus, we write

$$\hat{c} = \hat{c}_0, \quad \hat{h} = \hat{h}_0 \qquad \text{at} \qquad \hat{t} = 0. \tag{5}$$

We note that, for situations of practical interest, $\hat{c}_0 < \hat{c}_{\text{eq}}$. To summarise, equations (1) and (2) with boundary conditions (3) and (4), and initial conditions (5) form a closed system for the concentration of water and the height of the film.

2.1 Steady State

Before proceeding, we look for the steady-state solutions $\hat{c}_{ss} = \hat{c}_{ss}(\hat{x})$ and $\hat{h}_{ss} = \hat{h}_{ss}(\hat{x})$ to (1)–(5). Equation (2) tells us that

$$\hat{c}_{ss}|_{\hat{x}=\hat{h}} = \hat{c}_{\text{eq}}, \tag{6}$$

which we use to solve (1) along with (4) to find that

$$\hat{c}_{ss} = \hat{c}_{\text{eq}}. \tag{7}$$

We appeal to conservation of mass of sulphuric acid in order to find the final thickness of the liquid layer. Denoting by $\hat{N}$ the total initial moles of substance present in the layer, and the total number of moles of sulphuric acid by $\hat{S}$, we have that

$$\hat{S} = \hat{N} - \hat{A}\hat{c}_0\hat{h}_0 \qquad \text{at} \qquad \hat{t} = 0, \tag{8}$$

where $\hat{A}$ is the cross-sectional area of the layer, measured in m^2.

Once the system has settled into the steady state, since the change in thickness of the water layer is due purely to the increase in water molecules, the total number of moles of

sulphuric acid is given by

$$\hat{S} = \hat{N} - \hat{A}\hat{c}_{\mathrm{eq}}\hat{h}_{ss} + \frac{\hat{A}(\hat{h}_{ss} - \hat{h}_0)}{\hat{V}_m}. \tag{9}$$

Equating (8) and (9) and rearranging, we find that

$$\hat{h}_{ss} = \frac{\hat{h}_0(1 - \hat{V}_m\hat{c}_0)}{1 - \hat{V}_m\hat{c}_{\mathrm{eq}}}. \tag{10}$$

We note that the steady-state layer thickness is independent of the mass transfer coefficient $\hat{k}$.

2.2 Dimensionless Model

In order to find the key parameters that determine the behaviour of the system, we non-dimensionalise (1)–(5) using the following scalings

$$\hat{c} = \hat{c}_{\mathrm{eq}}c, \quad (\hat{x}, \hat{h}) = \hat{h}_0(x, h), \quad \hat{t} = (\hat{h}_0^2/\hat{D})t, \tag{11}$$

where we have chosen to scale with the timescale associated with diffusion across the layer (rather than the timescale associated with the interface motion). This proves useful when comparing our model with experimental results as we have a good estimate of both $\hat{h}_0$ and $\hat{D}$. Furthermore, we have chosen $\hat{c}_{\mathrm{eq}}$ as the scale for $\hat{c}$, since this parameter remained the same in our experiments (we maintained the same relative humidity). The resulting dimensionless equations, together with the boundary and initial conditions, are

$$\frac{\partial c}{\partial t} = \frac{\partial^2 c}{\partial x^2}, \tag{12}$$

$$\frac{\mathrm{d}h}{\mathrm{d}t} = \sigma\,\mathrm{Sh}(1 - c|_{x=h}), \tag{13}$$

subject to

$$-\frac{\partial c}{\partial x} - c\frac{\mathrm{d}h}{\mathrm{d}t} = \mathrm{Sh}(c-1) \qquad \text{at} \qquad x = h(t), \tag{14}$$

$$-\frac{\partial c}{\partial x} = 0 \qquad \text{at} \qquad x = 0, \tag{15}$$

$$c = \delta, \quad h = 1 \qquad \text{at} \qquad t = 0, \tag{16}$$

where we have introduced three dimensionless parameter groups, namely,

$$\mathrm{Sh} = \frac{\hat{k}\hat{h}_0}{\hat{D}}, \qquad \sigma = \hat{c}_{\mathrm{eq}}\hat{V}_m, \qquad \delta = \frac{\hat{c}_0}{\hat{c}_{\mathrm{eq}}}. \tag{17}$$

Here, Sh is the Sherwood number for water absorption, which compares the mass transfer across the interface with the rate of water diffusion, σ represents the thickness change associated with the equilibrium concentration, and δ is the ratio of the initial concentration to the equilibrium concentration, assumed to be less than one (since the initial concentration is lower than the equilibrium concentration). We also note that $\sigma < 1$, since the equilibrium concentration of water is less than the molar concentration of water.

2.3 The Case of Small Sherwood Number

Although the problem (12)–(16) is not very difficult to solve numerically, it is nonetheless a moving-boundary problem that requires a careful treatment. Before solving numerically, we would like to gain insight into the qualitative behaviour of the solutions for limiting values of the Sherwood number, since this is the number that we do not know *a priori*. To that end, we consider the limit in which $\mathrm{Sh} \ll 1$, which will provide substantial simplifications to the problem. This limit corresponds to the situation when the rate of diffusion of water is much faster than the rate of water absorption, respectively. We treat both σ and δ as $O(1)$ parameters, so that our model has the richest structure. We also briefly discuss the large-Sherwood-number limit in the Supporting Information, where we are also able to make

some simplifications.

When $\mathrm{Sh} \ll 1$, we see from (13) that, in this case, the right-hand side becomes small, and, to a good approximation, the film does not grow. This is not surprising since, in this limit, the diffusion timescale is much shorter than the absorptive timescale. Moreover, if we solve (12)–(16) neglecting the terms multiplied by Sh, equation (14) tells us that the flux of water from the atmosphere is zero, and, thus, the concentration remains at its initial value. In order to explore the film growth, we rescale time by $t = \tau/\mathrm{Sh}$, where $\tau = O(1)$, which corresponds to using the absorptive timescale, on which diffusion happens very fast. With this scaling, the model becomes

$$\mathrm{Sh}\frac{\partial c}{\partial \tau} = \frac{\partial^2 c}{\partial x^2}, \tag{18}$$

$$\frac{\mathrm{d}h}{\mathrm{d}\tau} = \sigma(1 - c|_{x=h}), \tag{19}$$

subject to

$$-\frac{\partial c}{\partial x} - \mathrm{Sh}\, c\frac{\mathrm{d}h}{\mathrm{d}\tau} = \mathrm{Sh}(c-1) \qquad \text{at} \qquad x = h(\tau), \tag{20}$$

$$-\frac{\partial c}{\partial x} = 0 \qquad \text{at} \qquad x = 0, \tag{21}$$

$$c = \delta, \quad h = 1 \qquad \text{at} \qquad \tau = 0. \tag{22}$$

Neglecting terms of $O(\mathrm{Sh})$, we see that (18), (20), and (21) yield a spatially uniform solution

$$c = c(\tau). \tag{23}$$

Thus, diffusion acts fast enough that the water concentration is uniform in the bulk liquid, but is not in equilibrium, and this gives rise to film growth. In order to solve for $c(\tau)$, we integrate (18) across the layer, and apply (20) and (21) to find that

$$\frac{\mathrm{d}(ch)}{\mathrm{d}\tau} = 1 - c|_{x=h} = \frac{1}{\sigma}\frac{\mathrm{d}h}{\mathrm{d}\tau}. \tag{24}$$

Integrating (24) and applying (22) gives a relationship between c and h, namely,

$$c = \frac{h - 1 + \delta\sigma}{\sigma h}. \tag{25}$$

Substituting from (25) into (19), we arrive at an ordinary differential equation for h,

$$\frac{\mathrm{d}h}{\mathrm{d}\tau} = \frac{(\sigma - 1)h + 1 - \delta\sigma}{h}, \tag{26}$$

which has to be solved subject to (22). The implicit solution for h reads

$$\tau = \frac{1}{\sigma - 1}\left(h - 1 - \frac{1 - \delta\sigma}{\sigma - 1}\log\left(\frac{(\sigma - 1)h + 1 - \delta\sigma}{(1 - \delta)\sigma}\right)\right). \tag{27}$$

From (26), we see that, as $\tau \to \infty$, h tends to a steady-state thickness given by

$$h_{\mathrm{eq}} = \frac{1 - \delta\sigma}{1 - \sigma}, \tag{28}$$

and, consequently, that $c \to 1$. We note that (28) is the dimensionless version of (10) presented in §2.1. Equation (28) further simplifies to $h_{\mathrm{eq}} = 1/(1 - \sigma)$ when $\delta \ll 1$, providing a simple formula for the equilibrium film thickness in this regime. Since the leading-order result is independent of the Sherwood number and the behaviour is limited by mass transfer, any concentration dependence in the diffusivity would not affect the system behaviour.

3 Experimental Set-Up

We now describe the experiments that we have carried out in order to help us determine the crucial unknown parameter $\hat{k}$. The experimental set-up shown in figure 2a, consists of a cylindrical glass vial with a flat bottom and a O-ring seal joint at the top connected to an open tube with a O-ring seal joint at the bottom. The diameter of the vial is 2.5 cm and its height is approximately 4.5 cm. An ePTFE membrane is secured between the vial and the

tube using the O-ring and a metal clamp, which partitions the vial from the tube. A small

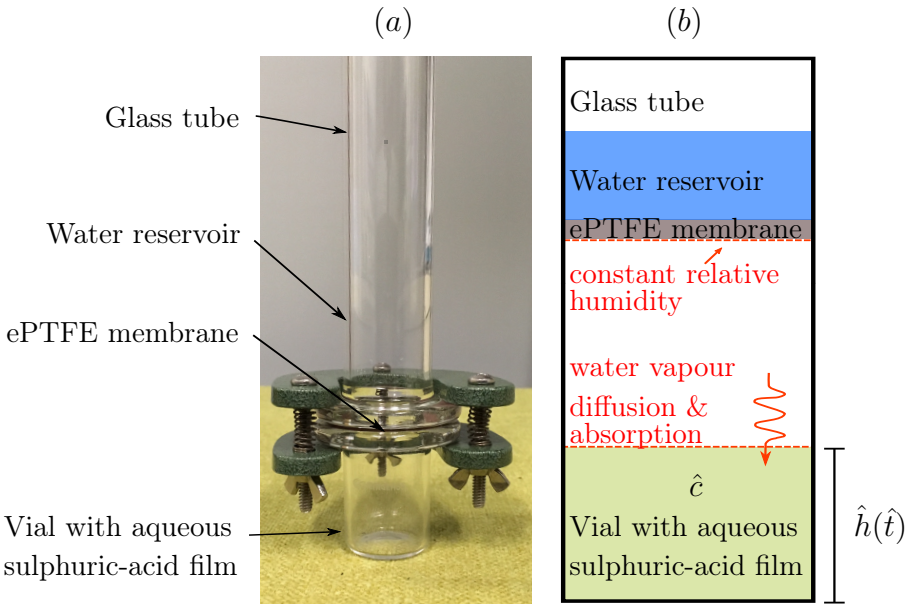

Figure 2: (a) Picture of the experimental set-up before filling it with liquid juxtaposed with (b) a schematic of the experiment.

amount of sulphuric acid with prescribed initial thickness and water concentration is placed in the vial (see table 1). The section above the membrane is filled with water to create a reservoir. The ePTFE membrane properties are such that liquid water does not penetrate and wet the membrane, but molecules of water vapour are free to diffuse through the porous structure. This set-up creates a constant-relative-humidity boundary at the bottom of the membrane surface. The overall set-up is shown schematically in figure 2b. The layer of sulphuric acid absorbs water vapour and, thus, creates a gradient in the bottom section of the vial that drives further diffusion of water molecules. Two experiments, each performed in two trials and lasting six months, were conducted at 95% relative humidity with the same thickness $\hat{h}_0 = 1.9 \times 10^{-3}\,\mathrm{m}$, but with two different starting concentrations, namely (a) $\hat{c}_0 = 3.6 \times 10^3\,\mathrm{mol\,m^{-3}}$ (concentrated acid) and (b) $\hat{c}_0 = 4.0 \times 10^4\,\mathrm{mol\,m^{-3}}$ (dilute acid). The water uptake was quantified by periodically measuring the weight of the acid solution in the vial (the measurements were taken 2–3 times a week in the first two months, and then once a week for the remaining four months of the experiment). Each measurement took

2–3 minutes and consisted of emptying the water from the glass tube (the acid was never removed from the vial), removing the top section, and weighing the bottom section (glass vial and liquid). The weight of the liquid is determined as the difference of the measured weight and the weight of the empty vial. The quantities of interest, namely, the sulphuric acid concentration and the film thickness, are then calculated from the initial concentration and weight uptake.

We list the known dimensional and dimensionless parameters for the two experiments in table 1 and table 2, and note that the absorption coefficient $\hat{k}$ and thus the Sherwood number Sh are unknown *a priori*.

Table 1: Dimensional parameters, taken from Wilson[16], Brini et al.[17], Leaist[18].

Parameter	Definition	Value	Units
$\hat{h}_0$	Initial liquid thickness	1.9×10^{-3}	m
$\hat{c}_0$	Initial water concentration	(a) 3.6×10^3, (b) 4.0×10^4	$\mathrm{mol\,m^{-3}}$
$\hat{A}$	Cross-section of glass vial	4.9×10^{-4}	$\mathrm{m^2}$
$\hat{c}_{\mathrm{eq}}$	Equilibrium water concentration[16]	5.4×10^4	$\mathrm{mol\,m^{-3}}$
$\hat{m}$	Molar mass of water[17]	1.8×10^{-2}	$\mathrm{kg\,mol^{-1}}$
$\hat{D}$	Diffusivity of water in aqueous sulphuric acid[18]	1.6×10^{-9}	$\mathrm{m^2\,s^{-1}}$
$\hat{V}_m$	Molar volume of water[17]	1.8×10^{-5}	$\mathrm{m^3\,mol^{-1}}$

Table 2: Dimensionless parameters.

Parameter	Value
σ	0.97
δ	(a) 0.067, (b) 0.74

4 Numerical Results

We now solve the full system (12)–(16) numerically and compare the results with the asymptotic reductions presented in §2.3. In order to solve the problem numerically, we map the time-dependent spatial domain $0 \leq x \leq h(t)$ to the fixed domain $0 \leq \xi \leq 1$ using the transformation $x = h(t)\xi$, discretise the system in space, and solve the problem using the

method of lines. In figure 3, we present the solutions for h and c for sample parameter values $\mathrm{Sh} = 1, \sigma = 0.5, \delta = 0.1$ in order to visualise the generic behaviour of the system, and, in particular, the saturation of the film thickness with time. We see that, in figure 3a, the film thickness evolves to an equilibrium value of 1.9, which agrees with the prediction from (28), while in figure 3b, we see that the water concentration first develops a moderate gradient near the gas–liquid interface due to water absorption before smoothing out as the concentration becomes uniform across the liquid film due to diffusion.

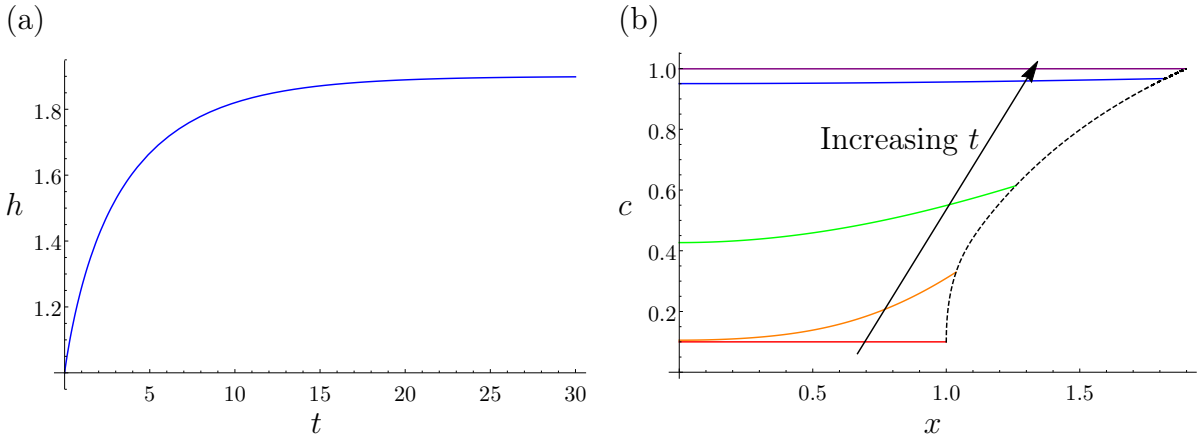

Figure 3: Graphs showing (a) the temporal profile of h, satisfying (12)–(16) and (b) the spatial profile of c for various times: $t = 0$ (red), 0.1 (orange), 1 (green), 10 (blue), 30 (purple). The position of the gas–liquid interface is shown with a dashed line. The parameters are $\sigma = 0.5$, $\mathrm{Sh} = 1$, and $\delta = 0.1$.

Having seen the general behaviour of the system, we now explore how the solution changes as the parameters change. Firstly, we vary $\hat{c}_{\mathrm{eq}}$, which changes both σ and δ, and the results are shown in figure 4a. We see that increasing $\hat{c}_{\mathrm{eq}}$ results in a larger equilibrium film thickness. This is because the larger the $\hat{c}_{\mathrm{eq}}$ the more water uptake is required to reach equilibrium. Secondly, we vary $\hat{c}_0$ by varying δ as shown in figure 4b. We see that increasing $\hat{c}_0$ leads to a decrease in the equilibrium film thickness. This is to be expected, since increasing $\hat{c}_0$ means that the initial concentration becomes closer to the equilibrium value $\hat{c}_{\mathrm{eq}}$, and so less water needs to be absorbed until equilibrium is reached. Thirdly, in figure 5, we present the film thickness versus time for various values of Sh between 1 and 0.1, and we see that there is excellent agreement between the numerical results and our asymptotic prediction

from §2.3, shown as a dashed line, as Sh $\to 0$. We note that we have plotted the results versus the scaled time τ to be consistent with the result in §2.3. Since changing Sh only alters the relative strength of reaction over diffusion, variations in this parameter determine the *approach* of the thickness to its equilibrium, including the time it takes to reach it, but not its actual value, which is given by (28).

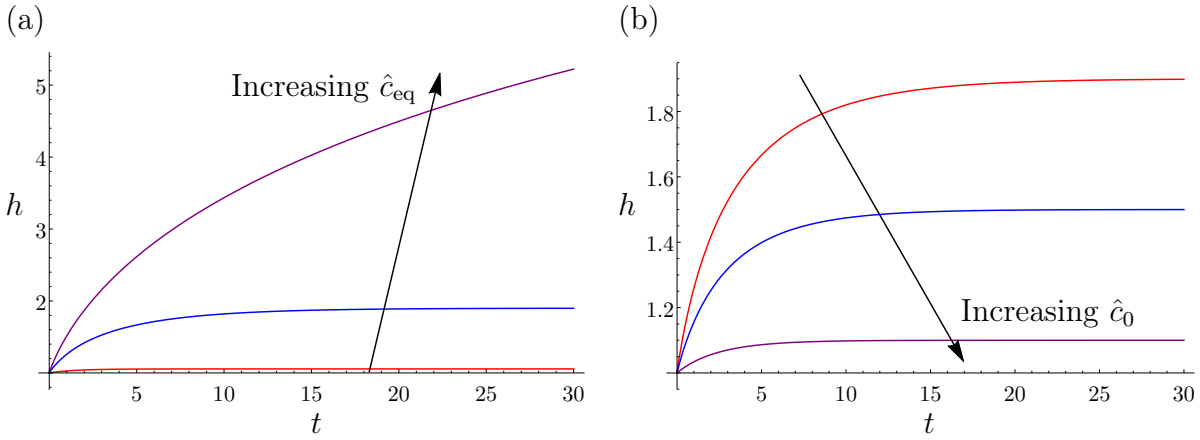

Figure 4: Graphs showing the temporal profile of h varying (a) $\hat{c}_{\text{eq}}$ by varying both (σ, δ): (0.1, 0.5) (red), (0.5, 0.1) (blue), (0.9, 0.06) (purple) and (b) $\hat{c}_0$ with $\delta = 0.1$ (red), 0.5 (blue), 0.9 (purple), with $\sigma = 0.5$. Here, Sh $= 1$.

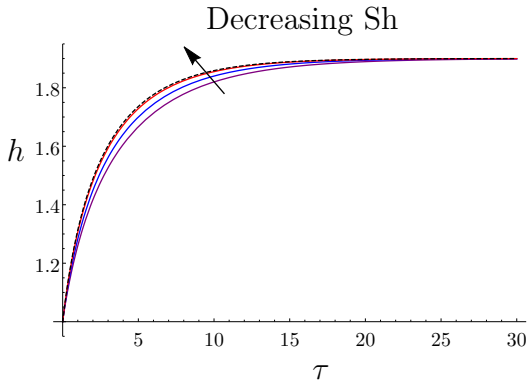

Figure 5: Graph showing how h varies with time for various values of Sh: Sh $= 1$ (purple), 0.5 (blue), 0.1 (red), asymptotic result from §2.3 (dashed). The other parameters are $\sigma = 0.5, \delta = 0.1$.

We also investigate the behaviour of the water concentration in the film in the limiting case of small Sh using the asymptotic reductions in §2.3. When Sh $\ll 1$, we see in figure 6 that, as discussed in §2.3, the concentration is spatially uniform across the film for all time under the influence of the dominating diffusion process, and equilibrium at the interface is

reached over a longer timescale.

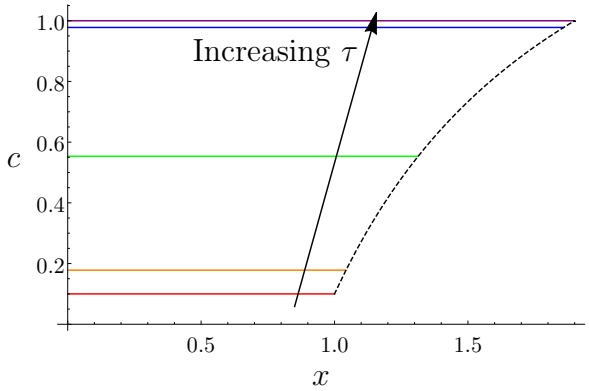

Figure 6: Graph showing how c varies with x for the small-Sh limit from §2.3 for various times: $\tau = 0$ (red), 0.1 (orange), 1 (green), 10 (blue), 30 (purple); the position of the gas–liquid interface is shown with a dashed line. The other parameters are $\sigma = 0.5$, $\delta = 0.1$.

Finally, we compare our numerical results against experimental data. We use the experiments with initial water concentration $\hat{c}_0 = 3.6 \times 10^3 \mathrm{mol\,m^{-3}}$ to determine the Sherwood number, which we find by fitting the experimental values of the mass, $\hat{M}$, of water in the liquid layer against

$$\hat{M}(\hat{t}) = \hat{m}\hat{A}\int_0^{\hat{h}(\hat{t})} \hat{c}\,\mathrm{d}\hat{x} = \hat{m}\hat{A}\hat{c}_{\mathrm{eq}}\hat{h}_0\int_0^{h(t)} c\,\mathrm{d}x, \tag{29}$$

where $\hat{m}$ is the molar mass of pure water (measured in $\mathrm{kg\,mol^{-1}}$). Using least squares, our fitting procedure gives that $\mathrm{Sh} = 0.1$, and we show the comparison between the dimensional data, the output of our model, and our small-Sh formula in figure 7a. We then use the fitted value of Sh to make a prediction when $\hat{c}_0 = 4.0 \times 10^4 \mathrm{mol\,m^{-3}}$, and we show the results from the model, the small-Sh approximation, and the dimensional experimental data in figure 7b. We see excellent agreement, which validates our model. We use the fitted value of the Sherwood number to determine the value of the parameter $\hat{k}$, which we find to be $\hat{k} = 8.8 \times 10^{-8} \mathrm{m\,s^{-1}}$ (at this value of the relative humidity). A similar order of magnitude was found for the equivalent coefficient for ternary systems of aluminium chlorohydrate, glycerol and water in Hennessy et al. [12].

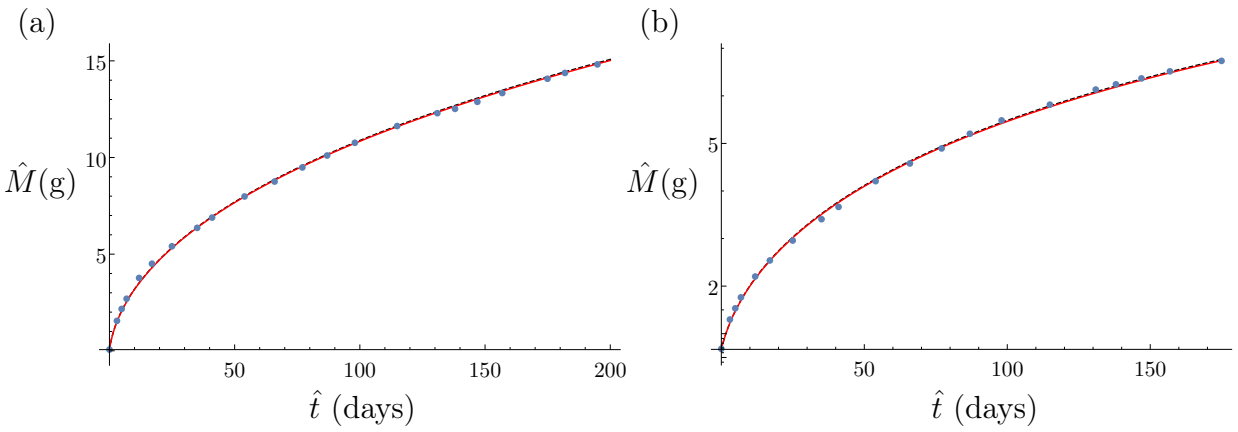

Figure 7: Graphs showing how $\hat{M}$, measured in g, varies with time, measured in days, (red) compared with the asymptotic result from §2.3 (dashed) and experimental data (blue dots) for (a) $\hat{c}_0 = 3.6 \times 10^3\,\mathrm{mol\,m^{-3}}$ with $\sigma = 0.97, \delta = 0.74$, and (b) $\hat{c}_0 = 4.0 \times 10^4\,\mathrm{mol\,m^{-3}}$ with $\sigma = 0.97, \delta = 0.067$. We fit the data to the model to find $\mathrm{Sh} = 0.1$.

5 Discussion and Conclusions

In this paper, we derived a one-dimensional model to describe the tendency of sulphuric acid to absorb water from its environment. We considered a uniform liquid film of aqueous sulphuric acid residing on an impermeable substrate which absorbs water through its surface from a constant-relative-humidity environment above. We assumed that the rate of absorption of water vapour is proportional to the difference between the water concentration at the surface and the equilibrium concentration. We identified three dimensionless numbers. Two of these correspond to properties that are easily measured experimentally, and involve the initial and equilibrium water concentrations. The third, the Sherwood number, is the ratio between the absorption rate and the diffusion rate, which cannot be extracted from a direct experimental measurement without using a model. We used the model to make a simple prediction about the final thickness of the liquid layer. In the small-Sherwood-number regime, we found that diffusion dominates over the reaction, and the concentration of water is spatially uniform across the liquid layer. We obtained an explicit solution for the film thickness and concentration in this regime. We solved the full system of equations numerically, explored the behaviour of the system as the parameters vary, and observed an excellent agreement with our asymptotic prediction in the appropriate limit.

We compared our results to experimental data from two experiments, namely, high and medium initial concentration of sulphuric acid at close to 100% relative humidity. The mathematical model gave excellent agreement in both cases for a fit to a single absorption coefficient, $\hat{k} = 8.8 \times 10^{-8}\,\mathrm{m\,s^{-1}} = 0.1$ mm day^{-1}, validating the model and determining the previously unknown value of $\hat{k}$. The model can now be used, with this value of $\hat{k}$, with confidence in other settings.

The diffusivity of water in sulphuric acid in our experiment varies between 1.2×10^{-9} and 2.0×10^{-9} m^{2}s^{-1}, according to Leaist [18], Umino and Newman [19]. If we use these values of $\hat{D}$ along with the fitted value for Sh, our range of estimates for $\hat{k}$ is $6.6 \times 10^{-8} - 11 \times 10^{-8}$ ms^{-1}. The associated Sherwood number was small, and the data was also well fitted using the small-Sherwood-number results. This suggests that our simple analytical solution (27) can be used to predict the amount of absorbed water without having to solve any differential equations numerically. To test the model predictions further it would be useful to perform more experiments with different values of the relative humidity, but we acknowledge that these are difficult to carry out.

A simplifying assumption we made was that the water diffusivity was constant throughout an experiment. In practice this diffusivity can vary with sulphur dioxide concentration. However, we found that concentration-dependent variations in diffusivity play no role in the small-Sherwood-number limit of interest, since here the behaviour is limited by mass transfer. In the Supplementary Information, our preliminary study shows that a concentration-dependent diffusivity also has little effect on the system behaviour for larger Sherwood numbers. However, a more comprehensive study of the effects would be worthwhile. Further, since the absorption of water is an exothermic reaction, we are also interested in relaxing our isothermal assumptions and incorporating heat transfer into our model. In both these cases, small changes may become important if lateral temperature or concentration gradients are established at the liquid-gas interface, since these can generate significant Marangoni flows. In such cases, our one-dimensional approximation would break down and we would need to

consider the two-dimensional analogue and incorporate the fluid flow.

~~The generality of~~ Our simple model ~~means that it~~ can be readily used for other systems where water or indeed other substances are absorbed from the environment before diffusing through a liquid film. Examples include alcohols, such as ethanol, methanol, glycerol, and also sodium hydroxide, paints, and coatings.

Our experimental results showed that there was a seven-fold increase in the thickness of the sulphuric acid layer by the end of our six-month-long experiment (figure 6), confirming the severity of volume change by this mechanism and that hygroscopy will play a key role in sulphuric acid layer growth in industrial settings. Our future aim is to use the model presented in this paper to incorporate the effect of hygroscopy into our model[20] for chemical filtering devices for suplhur dioxide, in order to understand the importance of water absorption on device performance.

Acknowledgement

This publication is based on work partially supported by the EPSRC Centre For Doctoral Training in Industrially Focused Mathematical Modelling (EP/L015803/1) in collaboration with W. L. Gore and Associates, Inc. IMG gratefully acknowledges support from the Royal Society through a University Research Fellowship.

Supporting Information Available

Asymptotic and numerical results for the thickness and concentration in the large-Sherwood-number limit.

References

(1) House, J. E. *Inorganic Chemistry*, 2nd ed.; Academic Press, 2013; pp 517–520.

(2) Perry, R. H. In *Perry's Chemical Engineers' Handbook*, 7th ed.; Green, D. W., Maloney, J. O., Eds.; McGraw-Hill: New York, 1997.

(3) Joshi, B. K.; Kandpal, N. D. Volumetric and transport properties of aqueous sulphuric acid. *Phys. Chem. Liq.* **2007**, *45*, 463–470.

(4) Sippola, H.; Taskinen, P. Thermodynamic properties of aqueous sulfuric acid. *J. Chem. Eng. Data* **2014**, *59*, 2389–2407.

(5) Lewis, W. K.; Whitman, W. G. Principles of gas absorption. *J. Ind. Eng. Chem.* **1924**, *16*, 1215–1220.

(6) Greenewalt, C. H. Absorption of water vapor by sulfuric acid solutions. *J. Ind. Eng. Chem.* **1926**, *18*, 1291–1295.

(7) Zhou, J.; Tee, T. Y.; Zhang, X.; Luan, J. E. Characterization and modeling of hygroscopic swelling and its impact on failures of a flip chip package with no-flow underfill. In *Proceedings of the 2005 7th Electronics Packaging Technology Conference*. IEEE, 2006; pp 561–568.

(8) Delgado, J. M.; Ramos, N. M.; De Freitas, V. P. Can moisture buffer performance be estimated from sorption kinetics? *J. Build. Phys.* **2006**, *29*, 281–299.

(9) Hsu, H. C.; Hsu, Y. T.; Hsich, W. L.; Weng, M. C.; ZhangJian, S. T.; Hsu, F. J.; Chen, Y. F.; Fu, S. L. Hygroscopic swelling effect on polymeric materials and thermo-hygro- mechanical design on finger printer package. *2008 3rd International Microsystems, Packaging, Assembly and Circuits Technology Conference, IMPACT* **2008**, 291–294.

(10) Canuto, H. M. P.; Afonso, M. R. A.; da Costa, J. M. C. Hygroscopic behavior of freeze-dried papaya pulp powder with maltodextrin. *Acta Scientiarum-Technology* **2013**, *36*, 179–185.

(11) Sweijen, T.; van Duijn, C. J.; Hassanizadeh, S. M. A model for diffusion of water into a swelling particle with a free boundary: Application to a super absorbent polymer particle. *Chem. Eng. Sci.* **2017**, *172*, 407–413.

(12) Hennessy, M. G.; Ferretti, G. L.; Cabral, J. T.; Matar, O. K. A minimal model for solvent evaporation and absorption in thin films. *J. Colloid Interface Sci.* **2017**, *488*, 61 – 71.

(13) Alfrey, J., T.; Gurnee, E.; Lloyd, W. Diffusion in glassy polymers. *J. Polym. Sci. C* **1966**, *12*, 249 – 261.

(14) Cohen, D. S.; Erneux, T. Free boundary problems in controlled release pharmaceuticals. I: Diffusion in glassy polymers. *SIAM J. Appl. Math.* **1988**, *48*, 1451 – 1465.

(15) Mitchell, S.; O'Brien, S. Asymptotic, numerical and approximate techniques for a free boundary problem arising in the diffusion of glassy polymers. *Appl. Math. Comput.* **2012**, *219*, 376 – 388.

(16) Wilson, R. E. Humidity control by means of sulfuric acid solutions, with critical compilation of vapor pressure data. *J. Ind. Eng. Chem.* **1921**, *13*, 326–331.

(17) Brini, E.; Fennell, C. J.; Fernandez-Serra, M.; Hribar-Lee, B.; Lukšič, M.; Dill, K. A. How water's properties are encoded in its molecular structure and energies. *Chem. Rev.* **2017**, *117*, 12385–12414.

(18) Leaist, D. G. Diffusion in aqueous solutions of sulfuric acid. *Can. J. Chem.* **1984**, *62*, 1692–1697.

(19) Umino, S.; Newman, J. Diffusion of sulfuric acid in concentrated solutions. *J. Electrochem. Soc.* **1993**, *140*, 2217–2221.

(20) Kiradjiev, K.; Breward, C.; Griffiths, I.; Schwendeman, D. A homogenised model for a reactive filter. *Submitted to SIAM J. Appl. Math.* **2019**,

For Table of Contents Only